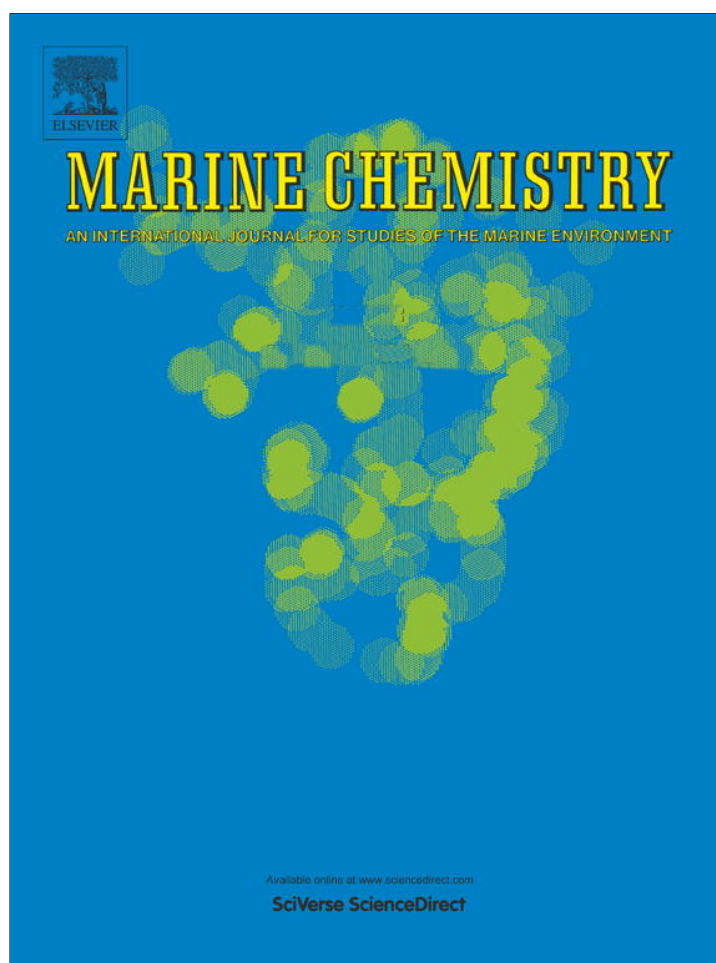


Provided for non-commercial research and education use.  
Not for reproduction, distribution or commercial use.



(This is a sample cover image for this issue. The actual cover is not yet available at this time.)

**This article appeared in a journal published by Elsevier. The attached copy is furnished to the author for internal non-commercial research and education use, including for instruction at the authors institution and sharing with colleagues.**

**Other uses, including reproduction and distribution, or selling or licensing copies, or posting to personal, institutional or third party websites are prohibited.**

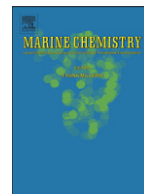
**In most cases authors are permitted to post their version of the article (e.g. in Word or Tex form) to their personal website or institutional repository. Authors requiring further information regarding Elsevier's archiving and manuscript policies are encouraged to visit:**

**<http://www.elsevier.com/copyright>**



Contents lists available at SciVerse ScienceDirect

## Marine Chemistry

journal homepage: [www.elsevier.com/locate/marchem](http://www.elsevier.com/locate/marchem)

# Measurement of $^{224}\text{Ra}$ : $^{228}\text{Th}$ disequilibrium in coastal sediments using a delayed coincidence counter

Pinghe Cai <sup>a,\*</sup>, Xiangming Shi <sup>a</sup>, Willard S. Moore <sup>b</sup>, Minhan Dai <sup>a</sup>

<sup>a</sup> State Key Laboratory of Marine Environmental Science, Xiamen University, Xiamen 361005, China

<sup>b</sup> Department of Earth and Ocean Sciences, University of South Carolina, Columbia, South Carolina 20208, USA

## ARTICLE INFO

## Article history:

Received 16 March 2012

Received in revised form 27 May 2012

Accepted 31 May 2012

Available online 9 June 2012

## Keywords:

$^{224}\text{Ra}$ : $^{228}\text{Th}$  disequilibrium

Coastal sediments

RaDeCC system

GEOTRACES

## ABSTRACT

We describe a method for measuring  $^{224}\text{Ra}$  and  $^{228}\text{Th}$  activities in coastal sediments based on a delayed-coincidence counting system (the RaDeCC system). Milli-Q water is added to bulk sediment to form a slurry.  $^{224}\text{Ra}$  in interstitial water is co-precipitated by  $\text{MnO}_2$  suspension. The  $\text{MnO}_2$  suspension and the sediment with absorbed  $^{224}\text{Ra}$  and  $^{228}\text{Th}$  are filtered onto a 142-mm 0.7  $\mu\text{m}$  (nominal pore size) GFF filter. The filter is placed onto a sample holder specified for sediment samples and counted in a RaDeCC system.  $^{224}\text{Ra}$  and  $^{228}\text{Th}$  activities are calculated from two measurements that are conducted within 6–12 h and in 8–10 days after sample collection. The RaDeCC system is calibrated with a  $^{232}\text{U}$ - $^{228}\text{Th}$  standard using the method of standard addition. The reproducibility and the overall accuracy of  $^{224}\text{Ra}$  and  $^{228}\text{Th}$  measurements based on this method are estimated to be  $\pm 5\%$  and  $\pm 5$ –7%, respectively. We have applied this method to a coastal sediment and observed a significant deficit of  $^{224}\text{Ra}$  with respect to  $^{228}\text{Th}$  in the upper 3–4 cm.

© 2012 Elsevier B.V. All rights reserved.

## 1. Introduction

Short-lived, naturally occurring radionuclides are powerful tools for tracing the processes related to sedimentation and early diagenesis in marine sediments (e.g., [Aller and Cochran, 1976](#); [Krishnaswami et al., 1980](#)). As a noble gas,  $^{222}\text{Rn}$  (half-life 3.83 days) is free of chemical and biological processes in marine environment and was first proposed as a potential tracer for exchange across the water-sediment interface by [Broecker \(1965\)](#). Utilization of  $^{222}\text{Rn}$  to investigate sediment irrigation and mixing was exploited by several researchers (e.g., [Hammond et al., 1977](#); [Smethie et al., 1981](#)). One complication, however, is that the  $^{222}\text{Rn}$  deficit with respect to its parent nuclide,  $^{226}\text{Ra}$ , in a sediment sample was generally assessed by a technique requiring creation of a slurry of water and sediment. This procedure increases  $^{222}\text{Rn}$  emanation from marine sediments by a variable amount, thereby making it difficult to assess the  $^{222}\text{Rn}$  deficit ([Berelson et al., 1982](#)).

An analog to  $^{222}\text{Rn}$  is the short-lived radium isotope,  $^{224}\text{Ra}$ . Its half-life (3.66 days) is very close to  $^{222}\text{Rn}$ . In marine environments,  $^{224}\text{Ra}$  is produced continuously from alpha decay of  $^{228}\text{Th}$  (half-life 1.91 years) that is strongly bound to sediments. In contrast to the highly particle-reactive  $^{228}\text{Th}$ ,  $^{224}\text{Ra}$  exhibits dramatically different geochemical characteristics in freshwater and seawater. In freshwater,  $^{224}\text{Ra}$  is bound strongly onto particle surfaces; however, as the ionic strength increases during mixing into seawater, desorption occurs and some  $^{224}\text{Ra}$  is released ([Swarzenski et al., 2003](#)). Similar

processes take place in marine sediments, whereby  $^{224}\text{Ra}$  actively migrates across the sediment–water interface into the overlying seawater. As a consequence, disequilibrium between  $^{224}\text{Ra}$  and  $^{228}\text{Th}$  in near-surface sediments is anticipated.

Historically, measurements of  $^{224}\text{Ra}$  were conducted mostly in water samples. These measurements have enabled researchers to gain valuable knowledge on estuarine/ocean mixing, submarine groundwater discharge and water/soil interaction (e.g., [Moore, 2000](#); [Charette et al., 2001](#); [Krest and Harvey, 2003](#); [Kim et al., 2008](#)). However, due to analytical difficulties, few measurements of  $^{224}\text{Ra}$  have been performed on marine sediments ([Sun and Torgensen, 2001](#)). In this study, we describe a new method for determining  $^{224}\text{Ra}$  and  $^{228}\text{Th}$  on bulk sediment. On the basis of this method, we report the first robust measurement of  $^{224}\text{Ra}$ : $^{228}\text{Th}$  disequilibrium in coastal sediments.

## 2. Analytical method

Our method is based on a delayed-coincidence counting system (the RaDeCC system) that has been widely adopted to determine  $^{224}\text{Ra}$  and  $^{223}\text{Ra}$  in seawater ([Moore and Arnold, 1996](#); [Moore, 2008](#)). The RaDeCC system monitors alpha decays of the short-lived Rn daughters of  $^{224}\text{Ra}$  and  $^{223}\text{Ra}$ , which recoil from the  $\text{MnO}_2$  fiber. In this study, we have modified the sample chamber to replace the  $\text{MnO}_2$  fiber with a sediment sample. This sample chamber is designed to accommodate a 142 mm GF/F filter ([Fig. 1](#)). With an inner height of 3.0 mm, the chamber has a volume of 47.5  $\text{cm}^3$ . Inlet and outlet tubes are on the end opposite the chamber. We use 4.0-mm inner diameter

\* Corresponding author. Tel.: +86 592 2182811; fax: +86 592 2180655.  
E-mail address: [caiph@xmu.edu.cn](mailto:caiph@xmu.edu.cn) (P. Cai).

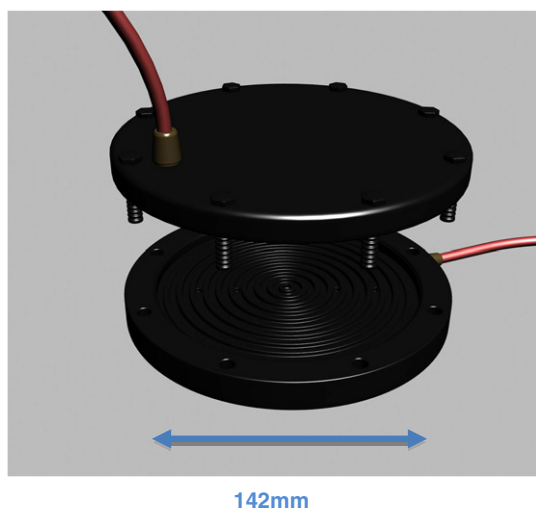


Fig. 1. Illustration of the sample chamber constructed for sediment samples.

tubes to connect the RaDeCC circulation system. This reduced the dead volume to <5% of the > 1 L total system volume.

The analytical procedure for  $^{224}\text{Ra}$  and  $^{228}\text{Th}$  on bulk sediments is as follows. Cores were taken either from a box corer ( $20 \times 20 \times 60$  cm) or by directly inserting a 47-mm-diameter PVC tube into the sediment. The cores were checked to ensure that the interface was undisturbed. Within 30 min after sample collection, the cores were sliced into 1-cm thick slabs. In general, 8–12 samples were taken at various depths between 0 and 20 cm. The sediment was placed in a 250 ml Teflon beaker and 150 ml Milli-Q water was added. The sediment and Milli-Q water were mixed to form a slurry. The slurry was ultrasonicated for 5 min. To the slurry 5–10 drops of concentrated  $\text{NH}_3 \cdot \text{H}_2\text{O}$  were added, which changed the pH to 8.0–9.0. Then, 1.0 ml of  $\text{KMnO}_4$  solution ( $3.0 \text{ g l}^{-1}$ ) and 1.0 ml of  $\text{MnCl}_2$  solution ( $8.0 \text{ g MnCl}_2 \cdot 4\text{H}_2\text{O l}^{-1}$ ) were added to form a suspension of  $\text{MnO}_2$ , which serves to absorb dissolved  $^{224}\text{Ra}$  in interstitial water. Subsequently, the sediment slurry together with the  $\text{MnO}_2$  precipitate was filtered onto a pre-weighed 142-mm  $0.7 \mu\text{m}$  (nominal pore size) GFF filter. While filtering, the slurry was vigorously stirred to ensure that sediment particles were evenly distributed onto the filter. The filtration was terminated when droplets of water ceased to issue from the filter. Under this situation, sediment particles on the filter remained moist. The sample was then placed into the sample chamber and was dried for ~30 min using an air stream. After the weight ratio of water/(sediment + filter) was adjusted to 0.4–0.5, we recorded the weight of the sample and connected the sample chamber to the RaDeCC system. Helium was circulated through the sediment sample and the counting cell at a rate of 12–15 L/min. The sample was counted for 4–6 h. In general, this resulted in > 1000 counts in the 220 channel. After measurement, the sample was removed from the sample chamber and stored until the second measurement. During storage, the water content of the sample was maintained in the vicinity of the in-situ level by periodically spraying Milli-Q water onto the sediment surfaces. About 8–10 days later, the sample was re-measured using a same RaDeCC system. In order to minimize the error, measurement parameters (like water content, counting time, etc.) were controlled to be consistent with the first measurement.

We have also checked if there is a significant amount of residual  $^{224}\text{Ra}$  in the filtrate. Filtrates from a total of 3 sediment samples were combined, and 5.0 ml of  $\text{KMnO}_4$  solution and 5.0 ml of  $\text{MnCl}_2$  solution were added to form a suspension of  $\text{MnO}_2$ . The  $\text{MnO}_2$  precipitate was filtered onto a 142-mm  $0.7 \mu\text{m}$  GFF filter.  $^{224}\text{Ra}$  activity was measured following the procedure described above. The result showed that <1% of total  $^{224}\text{Ra}$  resides in the filtrate. This indicates that our procedure has quantitatively removed all the  $^{224}\text{Ra}$  onto the GFF filter.

In our procedure, a third measurement for  $^{224}\text{Ra}$  after ~25 days is not compulsory as the time interval of 8–10 days has allowed > 75% of  $^{224}\text{Ra}$  deficit to grow toward equilibrium. Furthermore,  $^{228}\text{Th}$  activity should change by <1% in this time interval, thereby eliminating the need to correct the decay or in-growth of  $^{228}\text{Th}$ . Thus, the final  $^{224}\text{Ra}$  and  $^{228}\text{Th}$  activities at the sampling time were calculated from the first and the second measurements. Chance coincidence and contributions from the 219 channel were corrected using the equations described in Moore and Arnold (1996) and Moore (2008). The errors associated with  $^{224}\text{Ra}$  and  $^{228}\text{Th}$  activities were propagated from counting statistics, counter calibration, chance coincidence correction and in-growth correction. In general, our procedure enables the first measurement to be accomplished within 6–12 h after sample collection. Under this situation, the error introduced by the initial in-growth correction of  $^{224}\text{Ra}$  is greatly reduced as it accounts for <10% of the total deficit of  $^{224}\text{Ra}$ .

It should be noted that  $^{224}\text{Ra}$  and  $^{228}\text{Th}$  activities measured via the RaDeCC system represents only the fraction absorbed on sediment surfaces. We have determined  $^{228}\text{Th}$  activities in the bulk sediment particles by using the traditional  $\alpha$ -spectrometric method (e.g., Cai et al., 2006). The result shows that  $^{228}\text{Th}$  absorbed on sediment surfaces accounts for ~30–40% of the total  $^{228}\text{Th}$  in sediment particles. It is the  $^{224}\text{Ra}$  produced from surface-absorbed  $^{228}\text{Th}$  that is involved in the exchange across the sediment–water interface. In this regard, it could be more appropriate to term the measured  $^{224}\text{Ra}$  and  $^{228}\text{Th}$  exchangeable  $^{224}\text{Ra}$  and production rate of exchangeable  $^{224}\text{Ra}$ , respectively. For convenience, however, hereafter we simply refer to them as  $^{224}\text{Ra}$  and  $^{228}\text{Th}$  activities.

### 3. Moisture and sample load experiments

Because we measure  $^{220}\text{Rn}$  in the RaDeCC system, we must ensure that it is released consistently from the sample matrix. The emanation of  $^{220}\text{Rn}$  from the sample matrix is known to be controlled by the recoil range of  $^{220}\text{Rn}$  in the medium on the matrix surface. Sun and Torgensen (1998a) have reported that a (water/ $\text{MnO}_2$  fiber) weight ratio of 0.3–1.0 creates a water film of  $0.9 \times 10^{-4}$ – $3.0 \times 10^{-4}$  cm on the  $\text{MnO}_2$  fiber. This water film effectively stops most of the  $^{220}\text{Rn}$  recoiled from the  $\text{MnO}_2$  fiber, which may otherwise be embedded in the adjacent  $\text{MnO}_2$  particles. Because  $^{220}\text{Rn}$  can readily diffuse from the water film into the helium stream, the emanation efficiency of  $^{220}\text{Rn}$  reaches a maximum in this range of (water/ $\text{MnO}_2$  fiber) weight ratio. In the present study, we have evaluated the effect of water content of sediment samples on  $^{224}\text{Ra}$  measurement. As shown in Fig. 2,  $^{220}\text{Rn}$  emanation efficiency approaches a maximum when the water/sediment weight ratio is ~0.1. With continued increases in water content,  $^{220}\text{Rn}$  emanation efficiency decreases steadily. However, it is notable that when the water/sediment ratio is in the range of ~0.4–0.5,  $^{220}\text{Rn}$  emanation is rather insensitive to the variation in water

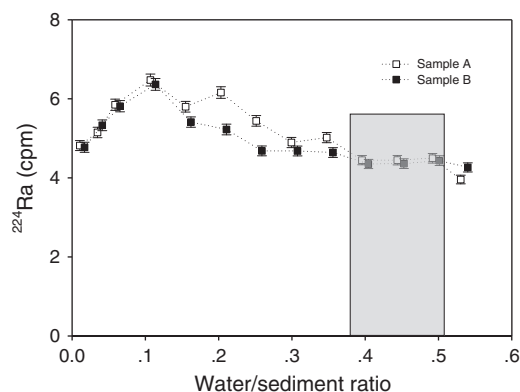


Fig. 2. A plot of apparent  $^{224}\text{Ra}$  activity vs. water/sediment ratio.

content. We did not further increase the water content, as it would create very “swampy” sediment on the filter, which could result in poor circulation of helium through the sample and hence cause significant measurement error. Our observation of the maximum  $^{220}\text{Rn}$  emanation at a water/sediment ratio of  $\sim 0.1$  is consistent with the previous study, which suggested that in this condition the sediment particles are covered with a water film close in thickness to the recoil range of  $^{220}\text{Rn}$  in water (Sun and Torgensen, 1998b). The decrease in  $^{220}\text{Rn}$  emanation for water/sediment ratio  $> 0.1$  could be due to the increase in the continuity of the water film (as ...water-particle-water-particle...). This would increase considerably the path length that  $^{220}\text{Rn}$  must diffuse to reach the circulating helium, much like the effect of the tortuosity in a sediment. For ease of the manipulation of water content, however, we have controlled the water/sediment ratio to be 0.4–0.5 during sample and standard measurements. As  $^{220}\text{Rn}$  emanation efficiency is quite stable at this level, any small variation in water content would not cause significant error in our  $^{224}\text{Ra}$  and  $^{228}\text{Th}$  measurements. Standards were measured using a similar water content (see below).

Due to the variation in porosity, the dried mass of the same volume of sediment from different depths or sites can vary dramatically. As such, we need to address how the sample load affects the  $^{224}\text{Ra}$  measurement. As shown in Fig. 3, a linear increase in the apparent  $^{224}\text{Ra}$  activity (cpm) is evident for sample loads in the range of 2–25 g. The linearity indicates that  $^{220}\text{Rn}$  emanation efficiency does not change significantly with sample load in this range. This linear increase in the apparent  $^{224}\text{Ra}$  activity, however, is not observed for sample loads  $> 25$  g, suggesting a significant reduction in  $^{220}\text{Rn}$  emanation efficiency. We suspected that the reduction in  $^{220}\text{Rn}$  emanation efficiency could be caused by the helium “channeling” in the sediment samples. This idea was testified by counting two sets of parallel sediment samples with different geometry. For the first set of samples ( $n = 2$ ), 20 g of sediment particles (dried weight) were evenly distributed onto a 142 mm GF/F filter. For the second set of samples ( $n = 2$ ), a same mass of sediment was distributed over only a half of the filter. Results show that the apparent  $^{224}\text{Ra}$  activity on the second set of samples is  $\sim 25\%$  lower than on the first set of samples ( $3.81 \pm 0.13$  cpm vs.  $5.17 \pm 0.28$  cpm,  $n = 2$ ; the associated uncertainty represents  $1\sigma$  standard deviation of the measurements on the replicate samples). This confirmed our idea that sample loads  $> 25$  g could increase helium “channeling” in the sample and lead to the reduction in  $^{220}\text{Rn}$  emanation efficiency. Therefore, we have controlled the sample loads to be  $< 25$  g during sample measurement.

#### 4. Calibration and reproducibility

The overall efficiency of the counting system is determined by measuring a set of standards in which known activities of  $^{224}\text{Ra}$  and

$^{228}\text{Th}$  were absorbed onto an unknown sediment sample. This is known as “the method of standard addition”. Normally, this method is used to solve the matrix effect problem. In doing so, natural sediment samples collected from the Yangtze River estuary were aged to achieve secular equilibrium between  $^{224}\text{Ra}$  and  $^{228}\text{Th}$ . The sediment samples were then mixed and homogenized. A set of 7 replicate samples each with a dried mass of 20.0 g were taken from the homogenized bulk sediment. To the replicate samples a succession (0.000, 1.000, 2.000, 3.000, 4.000, 5.000 and 6.000 ml) of  $^{232}\text{U}$ - $^{228}\text{Th}$  standard solutions with a  $^{228}\text{Th}$  activity of  $12.52 \pm 0.080$  dpm/ml were added. This standard solution had been stored for  $> 20$  years and thus  $^{232}\text{U}$ - $^{228}\text{Th}$ - $^{224}\text{Ra}$  should be in secular equilibrium. The  $^{228}\text{Th}$  activity of the solution was verified by  $\alpha$ -spectrometric analysis against a  $^{229}\text{Th}$  standard (NIST) in our lab. The samples were processed and measured following the procedure described in Section 2. The results of  $^{224}\text{Ra}$  measurement vs.  $^{228}\text{Th}$  addition from the standards are shown in Fig. 4. A simple Linear Least Square (LLS) analysis is performed using the SLOPE (y-array, x-array) and INTERCEPT (y-array, x-array) functions of SigmaPlot. The SLOPE gives the overall efficiency of the counting system. The associated uncertainty represents standard error, which is in the vicinity of 5–6% in this case.

The efficiency of the counting system derived using the method of standard addition was checked by a desorption experiment using aged sediment with  $^{224}\text{Ra}$  and  $^{228}\text{Th}$  in secular equilibrium. Seawater free of  $^{228}\text{Th}$  and  $^{224}\text{Ra}$  ( $^{228}\text{Th}$  activity  $< 0.005$  dpm/L,  $S = 34.62$ ) collected at  $\sim 3000$  m from the deep basin in the South China Sea was added to aged sediment to replace  $^{224}\text{Ra}$  from particle surfaces. After a three-step desorption, the seawater was separated from the sediment by centrifugation. The desorption experiment should create an appreciable deficit of  $^{224}\text{Ra}$  relative to  $^{228}\text{Th}$  in the sediment. The sediment was then used to prepare a sample following the abovementioned procedure and ingrowth of  $^{224}\text{Ra}$  was monitored (Fig. 5a). The desorbed  $^{224}\text{Ra}$  in the seawater was co-precipitated with  $\text{MnO}_2$  by the addition of 5.0 ml of  $\text{KMnO}_4$  solution and 5.0 ml of  $\text{MnCl}_2$  solution. Subsequently, the  $\text{MnO}_2$  precipitates were filtered onto a 142-mm GFF filter and the decay of  $^{224}\text{Ra}$  was monitored using a same RaDeCC system as used to measure sediment samples (Fig. 5b). The counting efficiency of the  $\text{MnO}_2$  precipitate was calibrated against a standard in which known activities of  $^{224}\text{Ra}$ - $^{228}\text{Th}$  were co-precipitated by a same amount of  $\text{MnO}_2$  precipitate. As shown in Fig. 5, within uncertainty the  $^{224}\text{Ra}$  ingrowth in the sediment sample is equal to the  $^{224}\text{Ra}$  activity on the  $\text{MnO}_2$  precipitate ( $2.08 \pm 1.14$  dpm vs.  $2.08 \pm 0.30$  dpm). This provides another check for the accuracy of the counting efficiency applied to sediment samples.

We have evaluated the reproducibility of the  $^{224}\text{Ra}$  measurements based on our method by repeatedly measuring, over a two weeks period, aged sediment samples with  $^{224}\text{Ra}$  and  $^{228}\text{Th}$  in secular equilibrium. Fig. 6 is a plot of sequential measurements of  $^{224}\text{Ra}$  on two sediment

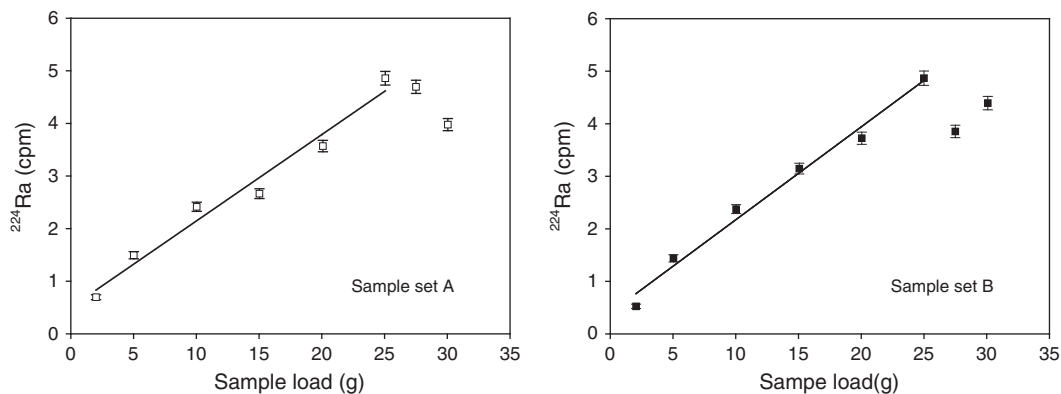
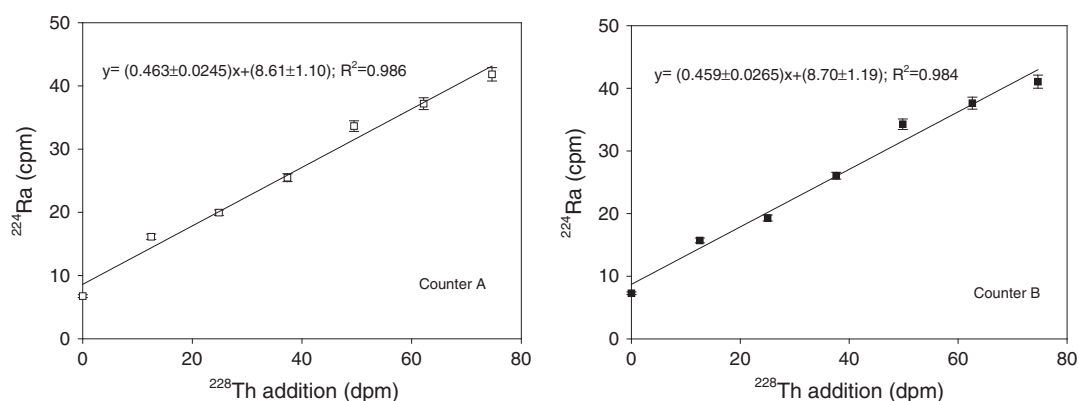


Fig. 3. Change of apparent  $^{224}\text{Ra}$  activity with sample load. Left panel is the result for sample set A and right panel for sample set B. The sample sets were taken from a homogenized bulk sediment. The water/sediment ratio was adjusted to 0.4–0.5 during measurement.



**Fig. 4.** Counting efficiency of the RaDeCC system derived using the method of standard addition. Left panel represents the result from RaDeCC system A and right panel from RaDeCC system B. Note that the water/sediment ratio was adjusted to 0.4–0.5 during sample measurement.

samples collected from the Yangtze River estuary. The error bar associated with each measurement represents  $\pm 1\sigma$  uncertainty propagated from counting statistics, chance coincidence correction and counter calibration. The sequential measurements gave mean  $^{224}\text{Ra}$  activities of  $12.9 \pm 0.48$  dpm and  $7.35 \pm 0.33$  dpm for sample A and sample B, respectively. The uncertainty represents 1 standard deviation and is within 5% of the measurements. This standard deviation is slightly lower than the  $\pm 1\sigma$  error associated with a single measurement ( $\pm 5$ –7%). It reflects the effect of the uncertainty in counter calibration on the overall accuracy of  $^{224}\text{Ra}$  measurement. Based on the above performance, we consider that our method is able to provide  $^{224}\text{Ra}$  and  $^{228}\text{Th}$  measurements on sediments with a reproducibility of  $\pm 5\%$  and an overall accuracy of  $\pm 5$ –7%.

### 5. Comparison of this technique with direct measurements on a slurry of the same sediment

We have compared our method with direct measurements on a slurry of the same sediment using the RaDeCC system. Aged, natural sediment samples collected from the Yangtze River estuary were mixed and homogenized. Two sets of 3 replicate samples each with a dried mass of 20.0 g were taken from the homogenized bulk sediment. For the first set ( $n=3$ ), samples were processed and measured in the same manner as described above. For the second set ( $n=3$ ), samples were processed in a way similar to the first set except that the step of the addition of  $\text{KMnO}_4$  and  $\text{MnCl}_2$  solutions was skipped. Results show that the  $^{224}\text{Ra}$  activity on the first set of samples is significantly higher than on the second set of samples ( $0.98 \pm 0.19$  dpm/g vs.  $0.74 \pm 0.07$  dpm/g,  $n=3$ ; the associated uncertainty represents  $1\sigma$  standard deviation of the measurements on the replicate samples). This

comparison demonstrates that Ra could effectively desorb from sediment surfaces during the creation of a sediment slurry. As such, the addition of  $\text{KMnO}_4$  and  $\text{MnCl}_2$  solutions is a necessity in the analytical procedure for measuring exchangeable  $^{224}\text{Ra}$  in coastal sediments.

### 6. Field application

We have performed  $^{224}\text{Ra}$  and  $^{228}\text{Th}$  measurement on natural samples in order to assess the applicability of our method. On 5 February 2011, short cores (10 cm in length and 4.7 cm in diameter) were taken at a site within Wuyuan Bay, Xiamen. This location is characterized by silty sediment. At high tide, it is covered with 0.5–1 m of seawater but at low tide, the sediment is exposed to the air. Bivalves are dominant benthic fauna at the study site. The cores were checked to ensure that the interface was undisturbed. Within 30 min after sample collection, the cores were transported to the laboratory and processed following the procedure described above. Fig. 7 shows the depth profile of  $^{224}\text{Ra}$  and  $^{228}\text{Th}$  activities in sediments. The  $^{224}\text{Ra}$  activity ranged from  $1.18 \pm 0.08$  dpm/g to  $1.98 \pm 0.15$  dpm/g (dried mass) and showed a minimum between 1 and 2 cm. In comparison, the  $^{228}\text{Th}$  activity varied between  $1.48 \pm 0.10$  dpm/g and  $2.03 \pm 0.12$  dpm/g and showed a minimum between 3 and 4 cm. In the upper 3–4 cm,  $^{224}\text{Ra}$  activity exhibited a significant deficit with respect to  $^{228}\text{Th}$ . Below this depth horizon,  $^{224}\text{Ra}$  and  $^{228}\text{Th}$  approached secular equilibrium. This distribution pattern is in accordance with our expectation that exchange between sediment and the overlying seawater generally takes place in the upper few centimeters of the sediment.

With a one-dimensional (1-D) exchange model, we calculated the  $^{224}\text{Ra}$  flux across the sediment–water interface using these  $^{224}\text{Ra}$  and  $^{228}\text{Th}$  measurements. The 1-D exchange model assumes: 1) that  $^{224}\text{Ra}$

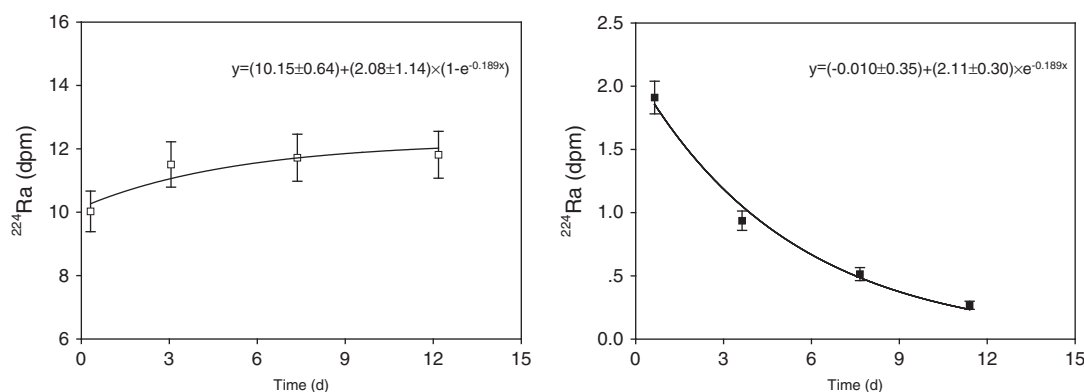


**Fig. 5.** Plots of in-growth of  $^{224}\text{Ra}$  with time in a sediment sample (left panel) and decay of  $^{224}\text{Ra}$  with time in a  $\text{MnO}_2$  precipitate sample (right panel). Note that the  $^{224}\text{Ra}$  in-growth in the sediment sample is equal to the  $^{224}\text{Ra}$  activity on the  $\text{MnO}_2$  precipitate ( $2.08 \pm 1.14$  dpm vs.  $2.11 \pm 0.30$  dpm).

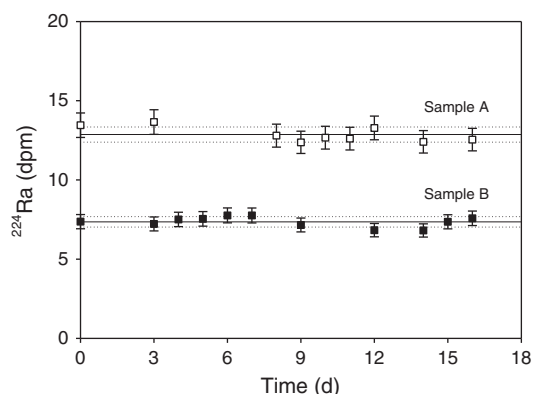


**Fig. 6.** Results of repeated counting of two sediment samples from the Yangtze River estuary. The solid lines represent the mean of the measurements and the dotted lines represent  $\pm 1$  standard deviation of the mean. Note that the samples were aged before measurement in order to achieve secular equilibrium between  $^{224}\text{Ra}$  and  $^{228}\text{Th}$ .

is solely produced by the in-situ decay of  $^{228}\text{Th}$  in sediment, i.e., there is no extra sources for  $^{224}\text{Ra}$  (such as submarine groundwater discharge, SGD) and lateral advection and diffusion can be neglected; 2) that  $^{224}\text{Ra}$  and  $^{228}\text{Th}$  are essentially in secular equilibrium below the sampling depth; and 3) that steady-state distributions of  $^{224}\text{Ra}$  and  $^{228}\text{Th}$  are present. Based on these assumptions, we can express the rate of change in  $^{224}\text{Ra}$  activity by the equation

$$\partial A_{\text{Ra}} / \partial t = 0 = A_{\text{Th}} \lambda_{\text{Ra}} - A_{\text{Ra}} \lambda_{\text{Ra}} - T_{\text{Ra}} \quad (1)$$

where  $A_{\text{Ra}}$  and  $A_{\text{Th}}$  are the activities of  $^{224}\text{Ra}$  and  $^{228}\text{Th}$ , respectively;  $\lambda_{\text{Ra}}$  is the decay constant of  $^{224}\text{Ra}$  ( $= 0.189 \text{ d}^{-1}$ );  $T_{\text{Ra}}$  is the rate at which  $^{224}\text{Ra}$  is transported to the overlying seawater by the exchange across sediment–water interface. Reformulating Eq. (1) and integrating  $T_{\text{Ra}}$  from the sediment–water interface to the base of the sampling region we obtain

$$F_{\text{Ra}} = \int_0^{\infty} T_{\text{Ra}} dz = \int_0^z \lambda_{\text{Ra}} (A_{\text{Th}} - A_{\text{Ra}}) dz \quad (2)$$

where  $F_{\text{Ra}}$  represents  $^{224}\text{Ra}$  flux across the sediment–water interface and  $z$  is the sampling depth. In this case,  $F_{\text{Ra}}$  was quantified by trapezoidal integration of the  $^{224}\text{Ra}$  deficit in the sampling region and to

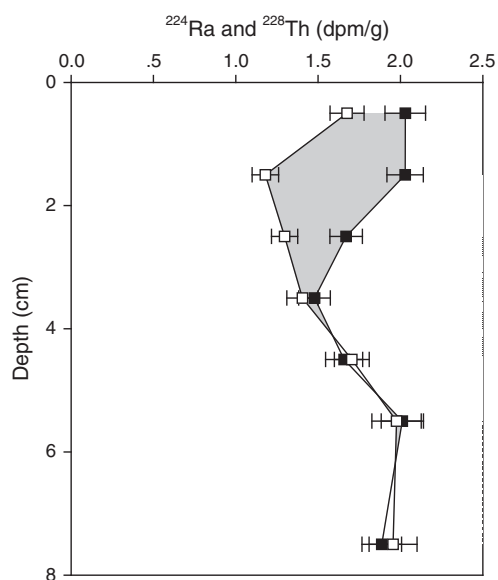


**Fig. 7.** Depth distribution of  $^{224}\text{Ra}$  (open square) and  $^{228}\text{Th}$  (filled square) in a sediment core from Wuyuan Bay, Xiamen. The shadowed area represents the deficit of  $^{224}\text{Ra}$ .

obtain a value of  $0.26 \pm 0.05 \text{ dpm cm}^{-2} \text{ d}^{-1}$ . In previous studies, Moore and Krest (2004) used a mass balance method for excess  $^{224}\text{Ra}$  in the bottom waters to estimate a  $^{224}\text{Ra}$  flux of  $0.05 \text{ dpm cm}^{-2} \text{ d}^{-1}$  from the sediment over the shelf of the Gulf of Mexico. In Great South Bay, New York, Beck et al. (2008) reported a  $^{224}\text{Ra}$  flux of  $0.0053 \text{ dpm cm}^{-2} \text{ d}^{-1}$  from the sediment based on core incubation experiments. In comparison, our value is about 1–2 orders of magnitude higher than these previous estimates. This probably reflects the differences in the physical conditions, biological mixing rates and sediment mineralogy between the study sites. Nonetheless, our result falls in the range of  $-26.4$ – $1.4 \text{ dpm cm}^{-2} \text{ d}^{-1}$  (the negative value represents a net scavenging of  $^{224}\text{Ra}$  by bottom sediments) that was derived using a diagenetic model for  $^{224}\text{Ra}$  in sediments (Sun and Torgensen, 2001).

## 7. Concluding remarks

The exchange across the sediment–water interface plays an important role in the biogeochemical cycling of major nutrients and trace metals in the coastal seas. Traditionally, this process was quantified by deploying an in-situ enclosure (i.e., benthic chamber) over the sediment to measure the flux into the overlying water, by modeling the depth profile of an element of interest in the sediment, or by constructing a mass balance for a substance in the water column. The first approach risks to bias the exchange by altering the physical conditions in the vicinity of the interface. The second approach is complicated by the effects of bottom currents and biological activities in the near-surface sediment. The third approach circumvents these difficulties. However, the application of this approach is not always possible because it generally requires a high spatial resolution of sample collection.

The disequilibrium of the mobile  $^{224}\text{Ra}$  with respect to  $^{228}\text{Th}$  that is strongly bounded on the surfaces of sediment particles is a most promising way to quantify the exchange across the sediment–water interface. This approach avoids the risk of altering the physical conditions near the sediment–water interface. In this study, we have developed a new method for measuring  $^{224}\text{Ra}$  and  $^{228}\text{Th}$  activities in coastal sediments based on a delayed-coincidence counting system. The method has been demonstrated to be very precise and rapid. It is able to provide  $^{224}\text{Ra}$  and  $^{228}\text{Th}$  measurements on sediments with a reproducibility of  $\pm 5\%$  and an overall accuracy of  $\pm 5$ – $7\%$ . In addition, the measurement can be conducted in the field within 6–12 h after sample collection. In combination with  $^{224}\text{Ra}$  measurement in the pore water, future application of  $^{224}\text{Ra}$ – $^{228}\text{Th}$  disequilibrium will enable researchers to quantify the exchange of major nutrients and trace metals (like DIC, Fe and Mn) across the sediment–water interface.

## Acknowledgments

This work was supported by the National Basic Research Program (“973” Program) of China through Grant No. 2009CB421203 and by the Natural Science Foundation of China (NSFC) through grant 41076041. Support to this work also came from the funds for creative research groups of the National Natural Science Foundation of China (Grant No. 41121091). Personal communication with Dr. Ken Buesseler at Woods Hole Oceanographic Institution inspired the design of the sample holder. Discussion with Dr. Guizhi Wang improved the quality of this paper. We thank Dr. M. M. Rutgers van der Loeff and an anonymous reviewer for their constructive comments.

## References

- Aller, R.C., Cochran, J.K., 1976.  $^{234}\text{Th}/^{238}\text{U}$  disequilibrium in near-shore sediment: particle reworking and diagenetic time scales. *Earth Planet. Sci. Lett.* 29, 37–50.
- Beck, A.J., Rapaglia, J.P., Cochran, J.K., Bokuniewicz, H.J., Yang, S., 2008. Submarine groundwater discharge to Great South Bay, NY, estimated using Ra isotopes. *Mar. Chem.* 109, 279–291.
- Berelson, W.M., Hammond, D.E., Fuller, C., 1982. Radon-222 as a tracer for mixing in the water column and benthic exchange in the southern California borderland. *Earth Planet. Sci. Lett.* 61, 41–54.

- Broecker, W.S., 1965. The application of natural radon to problems in ocean circulation. In: Ichiye, T. (Ed.), Symposium on diffusion in oceans and fresh waters. Lamont-Doherty Geological Observatory, Palisades, New York, pp. 116–145.
- Cai, P., Dai, M., Chen, W., Tang, T., Zhou, K., 2006. On the importance of the decay of  $^{234}\text{Th}$  in determining size-fractionated  $C/^{234}\text{Th}$  ratio on marine particles. *Geophys. Res. Lett.* 33, L23602, <http://dx.doi.org/10.1029/2006GL027792>.
- Charette, M.A., Buesseler, K.O., Andrews, J.E., 2001. Utility of radium isotopes for evaluating the input and transport of groundwater-derived nitrogen to a Cape Cod estuary. *Limnol. Oceanogr.* 46, 465–470.
- Hammond, D.E., Simpson, H.J., Mathieu, G., 1977. Radon-222 distribution and transport across the sediment–water interface in the Hudson River estuary. *J. Geophys. Res.* 82, 3913–3920.
- Kim, G., Ryu, J.-W., Hwang, D.-W., 2008. Radium tracing of submarine groundwater discharge (SGD) and associated nutrient fluxes in a highly permeable bed coastal zone, Korea. *Mar. Chem.* 109, 307–317.
- Krest, J.M., Harvey, J.W., 2003. Using natural distributions of short-lived radium isotopes to quantify groundwater discharge and recharge. *Limnol. Oceanogr.* 48, 290–298.
- Krishnaswami, S., Benninger, L.K., Aller, R.C., Von Damm, K.L., 1980. Atmospherically-derived radionuclides as tracers of sediment mixing and accumulation in near-shore marine and lake sediments: evidence from  $^7\text{Be}$ ,  $^{210}\text{Pb}$ , and  $^{239,240}\text{Pu}$ . *Earth Planet. Sci. Lett.* 47, 307–318.
- Moore, W.S., 2000. Determining coastal mixing rates using radium isotopes. *Cont. Shelf Res.* 20, 1993–2007.
- Moore, W.S., 2008. Fifteen years experience in measuring  $^{224}\text{Ra}$  and  $^{223}\text{Ra}$  by delayed-coincidence counting. *Mar. Chem.* 109, 188–197.
- Moore, W.S., Arnold, R., 1996. Measurement of  $^{223}\text{Ra}$  and  $^{224}\text{Ra}$  in coastal waters using a delayed coincidence counter. *J. Geophys. Res.* 101, 1321–1329.
- Moore, W.S., Krest, J., 2004. Distribution of  $^{223}\text{Ra}$  and  $^{224}\text{Ra}$  in the plumes of the Mississippi and Atchafalaya Rivers and the Gulf of Mexico. *Mar. Chem.* 86, 105–119.
- Smethie, W.M., Nittrouer, C.A., Self, R.F.L., 1981. The use of Radon-222 as a tracer of sediment irrigation and mixing of the Washington continental shelf. *Mar. Geol.* 42, 173–200.
- Sun, Y., Torgensen, T., 1998a. The effects of water content and Mn-fiber surface conditions on  $^{224}\text{Ra}$  measurement by  $^{220}\text{Rn}$  emanation. *Mar. Chem.* 62, 299–306.
- Sun, Y., Torgensen, T., 1998b. Rapid and sensitive measurement method for adsorbed  $^{224}\text{Ra}$  in sediments. *Mar. Chem.* 61, 163–171.
- Sun, Y., Torgensen, T., 2001. Adsorption-desorption reactions and bioturbation transport of  $^{224}\text{Ra}$  in marine sediments: a one-dimensional model with applications. *Mar. Chem.* 74, 227–243.
- Swarzenski, P.W., Porcelli, D., Andersson, P.S., Smoak, J.M., 2003. The behavior of U- and Th-series nuclides in the estuarine environment. *Rev. Mineral. Geochem.* 52, 577–606.